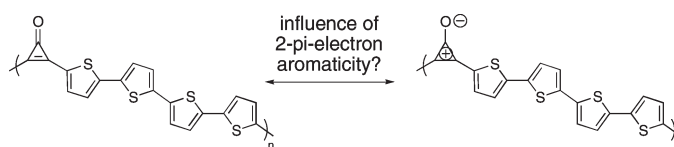# Poly(cyclopropenone)s: Formal Inclusion of the Smallest Hückel Aromatic into π-Conjugated Polymers[#]

Patricia A. Peart[†,§] and John D. Tovar[*,†,‡]

[†]Department of Chemistry and [‡]Department of Materials Science and Engineering, Johns Hopkins University, Baltimore, Maryland 21218. [§]Present address: Formulation Science; Dow Core R&D, Midland, MI.

tovar@jhu.edu

The synthesis of precursors to π-conjugated cyclopropenium polymers is described. Monomers for chemical and electrochemical manipulation are easily prepared through electrophilic substitution of in situ generated cyclopropenium cations that are then hydrolyzed to the respective cyclopropenones. The unusually strong dipole moment associated with the cyclopropenone renders this core formally aromatic, an electronic structure that becomes more important within individual monomers upon protonation of the carbonyl function with trifluoroacetic acid or alkylation with triethyloxonium salts. The electronic properties of cyclopropenone polymers in their pristine states and after acidification are discussed along with conjugated carbonyl-containing polymers that are also acid sensitive but without the added element of aromaticity. We find that the increased contributions of cyclopropenium cation aromaticity restrict the quinoidal charge carriers due to the energetically less favorable proposition of disrupting the local aromatic stabilization.

Introduction

The cyclopropenium cation has inspired substantial research on account of the unusual aromaticity associated with this two-π-electron motif, in essence the smallest Hückel aromatic. This molecule was first prepared by Breslow with three C_3-symmetrically disposed phenyl substituents and several years later as the unsubstituted parent ring structure.[1,2] There has since been a tremendous interest in the chemistry and properties of more complex molecular structures comprised of the cyclopropenium ion spanning synthetic and physical organic chemistry,[3,4] with uses extending into polystyrene modification,[5] alkynylated molecules as precursors to advanced materials,[6,7] photoacid-based initiators for cationic polymerizations,[8] and alcohol activation for nucleophilic substitution chemistry.[9] Although molecular examples are abundant, to our knowledge there are no reports that establish the properties of the cyclopropenium cation as a component of π-conjugated solution or solid-state polymeric electronic materials. We were attracted to these important π-electron building blocks in the context of our continuing interest in novel electronic polymers derived from classical Hückel aromatics.[10,11] We report here new studies of conductive polymers that incorporate two potential precursors to cyclopropenium cations: dichlorocyclopropenes and cyclopropenones. Our intentions were to examine the prospects for dissociative ionization and protonation (respectively) as a means to establish aromaticity within these two π-electron subunits and then examine the implications for charge transport in conjugated polymers that contain them.

[#]Taken in part from the Ph.D. thesis of P.A.P., Johns Hopkins, April 2010.
(1) Breslow, R. *J. Am. Chem. Soc.* **1957**, *79*, 5318.
(2) Breslow, R.; Groves, J. T.; Ryan, G. *J. Am. Chem. Soc.* **1967**, *89*, 5048.
(3) Krebs, A. W. *Angew. Chem., Int. Ed.* **1965**, *4*, 10–22.
(4) Komatsu, K.; Kitagawa, T. *Chem. Rev.* **2003**, *103*, 1371–1427.
(5) Weidner, C. H.; Long, T. E. *J. Polym. Sci., Part A: Polym. Chem.* **1995**, *33*, 1–6.
(6) Rubin, Y.; Knobler, C. B.; Diederich, F. *J. Am. Chem. Soc.* **1990**, *112*, 1607–1617.
(7) Gilbertson, R. D.; Weakley, T. J. R.; Haley, M. M. *J. Org. Chem.* **2000**, *65*, 1422–1430.
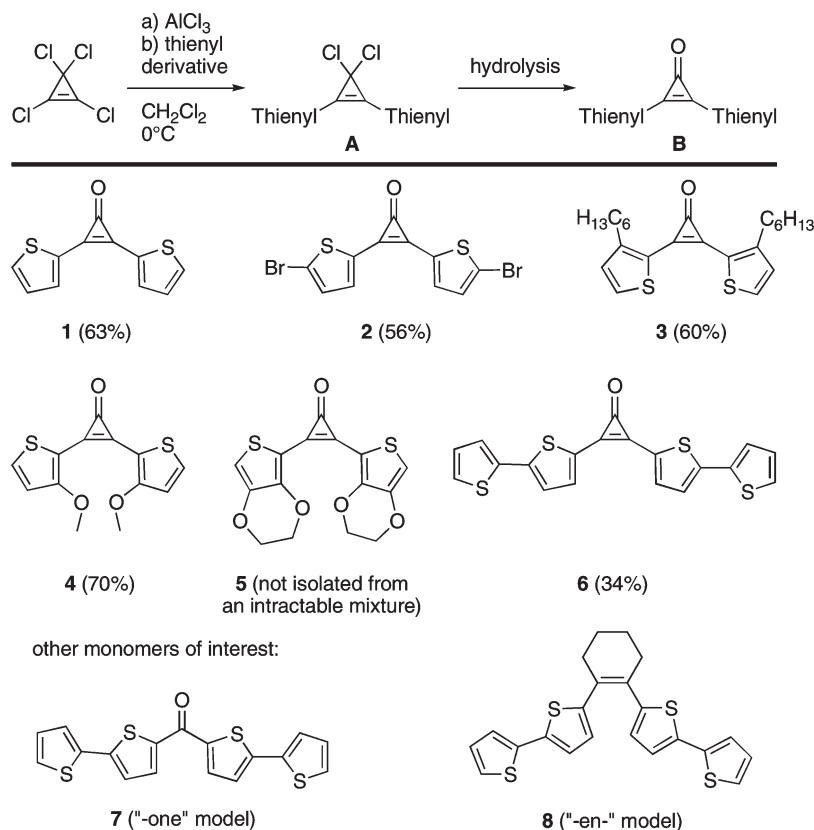
(8) Li, H. Y.; Ren, K. T.; Neckers, D. C. *Macromolecules* **2001**, *34*, 8637–8640.
(9) Kelly, B. D.; Lambert, T. H. *J. Am. Chem. Soc.* **2009**, *131*, 13930–13931.
(10) Peart, P. A.; Tovar, J. D. *Org. Lett.* **2007**, *9*, 3041–3044.
(11) Peart, P. A.; Tovar, J. D. *Macromolecules* **2009**, *42*, 4449–4455.

SCHEME 1. Synthesis of Thiophene-Containing Cyclopropenones via Friedel−Crafts-Type Arylation, and a Survey of Molecules Examined in This Work

1 (63%)   **2** (56%)   **3** (60%)

4 (70%)   **5** (not isolated from an intractable mixture)   **6** (34%)

other monomers of interest:

7 ("-one" model)   **8** ("-en-" model)

Results and Discussion

Monomer Syntheses. Attempts to prepare dichlorocyclopropene building blocks were enacted following the established electrophilic aromatic substitution routes of Komatsu et al. (Scheme 1).[12] The procedure involved treating tetrachlorocyclopropene with aluminum trichloride in dichloromethane to form trichlorocyclopropenium tetrachloroaluminate that was then treated with the appropriate thienyl compound to provoke a Friedel−Crafts-type of electrophilic attack. After aqueous workup, we found that the thienyl-substituted dichlorocyclopropenes (**A**) could be isolated but hydrolyzed very rapidly to the corresponding cyclopropenones (**B**). The ketones were thus treated with thionyl chloride, but the fleeting *gem*-dichlorinated structures again rapidly converted back to the cyclopropenones **B**. Since the cyclopropenone ring has substantial aromatic character,[13] we decided to use it as a formally aromatic surrogate building block for the two-π-electron aromatic cyclopropenium cation. Cyclopropenones have received substantial attention in their own right for example as masking agents for alkynes,[14,15] and as "aromatic" molecules due to the polarizability of the carbonyl double bond formally leading to a carbocation with a vacant p-orbital able to foster a ring current within the two π-electron monocycle. Scheme 1

depicts the synthesis route and thienyl-based cyclopropenone monomers **1−6** used for this study. The products were characterized by ^{1}H NMR, ^{13}C NMR, IR, and UV−vis spectroscopies as well as mass spectrometry.

Outside of Zefirov's recent work,[16] there are very few examples of heteroaromatic rings appended to cyclopropenone/cyclopropenium rings relative to the vast library of phenyl-substituted molecules. Furthermore, very little work has studied the oxidative electrochemistry of cyclopropenones to provide useful insights for electropolymerization strategies.[17] Therefore, we set out to expand the functional scope of the cyclopropenone core through the preparation of a variety of thiophene derivatives. The known compound **1** along with new derivatives that might be more amenable to chemical or electrochemical polymerization were prepared according to Scheme 1: brominated **2** has chemical handles for transition metal-mediated cross-couplings, hexylated **3** has solubilizing side chains, and molecules containing methoxy substituents (**4**), EDOTs (**5**), and bithiophenes (**6**) should have lower monomer oxidation potentials to facilitate oxidative polymerization. Remarkably, **2** could be synthesized from the reaction of the transient trichlorocyclopropenium cation with 2-bromothiophene without dehalogenation or polymerization. Although in principle the bromides of **2** should be reactive under typical transition metal-mediated cross-coupling conditions, Stille couplings performed in our laboratories have yielded as yet unidentified products in an

(12) Komatsu, K.; Tomioka, I.; Okamoto, K. *Tetrahedron Lett.* **1978**, 803–806.

(13) Salcedo, R.; Olvera, C. *THEOCHEM* **1999**, *460*, 221–230.

(14) Poloukhtine, A. A.; Popik, V. V. *J. Org. Chem.* **2003**, *68*, 7833–7840.

(15) Poloukhtine, A. A.; Mbua, N. E.; Wolfert, M. A.; Boons, G. J.; Popik, V. V. *J. Am. Chem. Soc.* **2009**, *131*, 15769–15776.

(16) Skornyakov, Y. V.; Lozinskaya, N. A.; Proskurnina, M. V.; Zefirov, N. S. *Russ. J. Org. Chem.* **2005**, *41*, 689–693.

(17) Cunha, S.; da Rocha, Z. N. *Quim. Nova* **2008**, *31*, 788–792.

SCHEME 2. Proposed Ionization Route To Obtain the Aromatic Cyclopropenium Ion within a Generic Conjugated Polymer Backbone
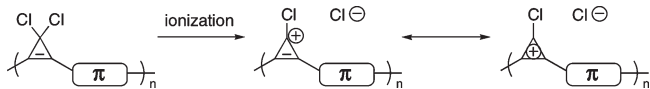

irreproducible manner, and we plan to explore the chemistry of this potentially powerful building block for monomer and polymer synthesis in future studies. Attempts to synthesize EDOT-appended **5** led to the formation of intractable materials, presumably the result of immediate and facile polymerization, and this molecule was not isolated. It was noted that in cases where the trichlorocyclopropenium cation could have been attacked through the 2 or 5 position of the thienyl reaction partner to give differing products (e.g., 3-hexylthiophene for **3** or 3-methoxythiophene for **4**), the major products turned out to be the symmetrical ones wherein substitution occurred regioselectively at the 2-position of the thiophene ring as determined by the characteristic thienyl coupling constants in the proton NMR. This result could be attributed to the fact that alkyl and alkoxy groups are electron-donating and activate the 2-positions for attack of the cyclopropenium electrophile.

We attempted the synthesis of dissected monomers shown in Scheme 1 bearing only the polarizable carbonyl (**7**, incorporating the "-one" portion of cyclopropenone)[18] and only the two-π-electron olefin fragment (**8**, the "-en-" portion) as model systems to understand the influence of the cyclopropenone ring and associated resonance contributors from zwitterionic structures. The "-one" model **7** was readily obtained through treating α-lithiobithiophene with dimethylcarbamyl chloride.[18] The "-en-" model **8** should have in principle been available through Pd-catalyzed cross-coupling chemistry, but its synthesis was problematic and the desired compound could not be obtained in pure form. We targeted the cyclic alkene over the simple *cis*-substituted ethene due to fears of olefin cis−trans isomerization during electrochemical polymerization.[19,20]

Aromaticity through Ionization. We initially envisioned the synthesis of cyclopropenyl polymers bearing labile chlorides with the intention to achieve charged substructures through a solvolysis-like pathway thus forming the aromatic cyclopropenium ring directly (Scheme 2). The initial dissociation of one of the chlorides would be facilitated by the energetic favorability to form an aromatic ring, and the resulting charged species could persist under the non-nucleophilic conditions typically employed for anodic organic electrochemistry rather than be attacked by nucleophilic solvents. The questions we were curious to probe involved conductivity properties of this charged aromatic as formed, and after continued electrochemical oxidation. Would this serve as a unique way to inject charge carriers within a conjugated polymer or would this be considered more as a localized aromatic cyclopropenium ring? Would this charged polymer once formed behave as a typical oligoaromatic or would there be a stronger donor−acceptor electronic character to it? Unfortunately this chloride dissociation route was met

SCHEME 3. Proposed Route To Obtain the Aromatic Cyclopropenium Ion through Carbonyl Protonation That Reinforces the Aromatic Character of the Cyclopropene Ring
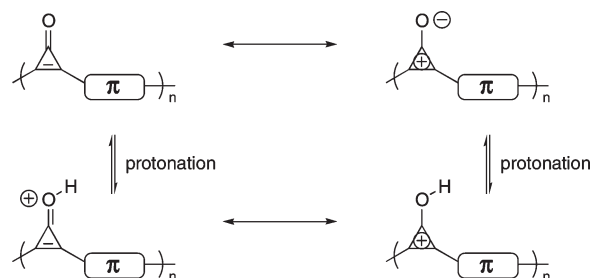
with difficulties. As a first test case, we prepared dithienyldichlorocyclopropene (Scheme 1, top), but as mentioned above, this molecule was too sensitive and underwent facile hydrolysis under ambient conditions within hours to the cyclopropenone **1**. We therefore abandoned this approach and turned our attention to cyclopropenone-containing polymers.

Aromaticity through Resonance/Protonation. The cyclopropenone ring system has an unusually basic carbonyl oxygen (and a substantial dipole moment) on account of the zwitterionic resonance contributor that places a formal negative charge on the oxygen while at the same time creating an electron deficiency on the carbon that can be compensated for through the establishment of an aromatic ring current in the carbocycle. The larger dipole moment of diphenylcyclopropenone (5.14 D) relative to benzophenone (3.0 D) would suggest enhanced basicity of the oxygen making up this highly polarized carbonyl bond.[21] This work is very much complementary to other contemporary efforts to explore carbonyl-containing cyclopentadienone (4 π-electron)[22,23] and tropone (6 π-electron)[24,25] units within conjugated polymer backbones. Similar to the tropone case, we expected that formal protonation of the cyclopropenone (presumably at the carbonyl oxygen) would lead to a resonance contributor with more aromatic character along the backbone of the conjugated polymer (Scheme 3). Here, we describe the electrochemical properties cyclopropenone monomers and the resulting conjugated polymers along with their spectroscopic and electrochemical alterations in the presence of acid and alkylating agents.

Monomer UV−Vis Spectroscopy. Among the cyclopropenone monomers of Scheme 1, **6** had the longest wavelength of maximum absorption (λ_{max}) as expected for the more conjugated bithiophene units. This was followed in order of decreasing λ_{max} by **4**, **3**, and **1**, a trend consistent with the HOMO−LUMO gaps calculated by DFT (B3LYP/6-31G*, Table 1). The cyclopropenone monomer **6** was red-shifted by 22 nm relative to the carbonyl-containing monomer **7** (λ_{max} at 398 nm). The addition of trifluoroacetic acid (TFA) to solutions of **1**, **3**, and **4** resulted in no notable shift in the λ_{max}, although the peak heights increased. The addition of TFA to

(18) Halvorsen, H.; Skramstad, J.; Hope, H. *Synth. Commun.* **2007**, *37*, 1179–1187.

(19) Onoda, M.; Iwasa, T.; Kawai, T.; Yoshino, K. *J. Phys. Soc. Jpn.* **1991**, *60*, 3768–3776.

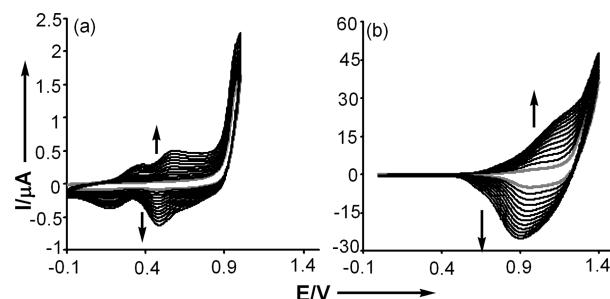(20) Berlin, A.; Zotti, G. *Synth. Met.* **1999**, *106*, 197–201.

(21) Breslow, R.; Eicher, T.; Krebs, A.; Peterson, R. A.; Posner, J. *J. Am. Chem. Soc.* **1965**, *87*, 1320–1325.

(22) Walker, W.; Veldman, B.; Chiechi, R.; Patil, S.; Bendikov, M.; Wudl, F. *Macromolecules* **2008**, *41*, 7278–7280.

(23) Yang, C.; Cho, S.; Chiechi, R. C.; Walker, W.; Coates, N. E.; Moses, D.; Heeger, A. J.; Wudl, F. *J. Am. Chem. Soc.* **2008**, *130*, 16524–16526.

(24) Takagi, K.; Nishikawa, Y.; Kunisada, H.; Yuki, Y. *Chem. Lett.* **2001**, 1244–1245.

(25) Sugiyasu, K.; Song, C.; Swager, T. M. *Macromolecules* **2006**, *39*, 5598–5600.

TABLE 1. DFT B3LYP/6-31G* Calculations and Experimental UV−Vis Data for Monomers

| monomer	HOMO (eV)	LUMO (eV)	HOMO−LUMO gap (eV, nm)	UV−vis (nm)
1	−5.99	−2.17	3.82, 325	269, 338, 356
3	−5.77	−2.03	3.74, 332	283, 345, 363
4	−5.24	−1.70	3.54, 350	285, 359, 378
6	−5.40	−2.48	2.92, 425	266, 332, 421, 442
7	−5.69	−2.33	3.36, 369	274, 398
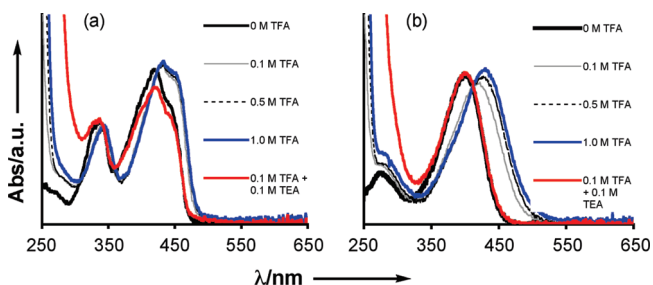
FIGURE 1. UV−visible spectra of (a) **6** and (b) **7** in chloroform solutions with different TFA concentrations and after neutralization of the acid with TEA.

FIGURE 2. Monomer CV of (a) cyclopropenyl **6** and (b) carbonyl **7** monomers recorded at 2 mm^2 Pt button working electrodes by cycling between 0 to 0.95 V (for a) and 0 to 1.4 V (for b) for 12 cycles at 100 mV/s scan rates in 2.5 mM monomer solutions in 0.1 M TBAPF$_6$/CH$_2$Cl$_2$ with potentials reported relative to Ag/Ag$^+$. The first scan is presented in gray.

the solutions of monomers **6** and **7** resulted in red-shifted λ_{max} values, with a more pronounced shift (30 nm) observed for carbonyl **7**. As the concentration of TFA was incrementally increased beyond 0.1 M, the red-shift observed for **7** was slight but noticeable while the absorption profile remained constant for the cyclopropenone **6** under the same conditions. Although TFA is a strong organic acid, it is important to realize that the equilibria shown in Scheme 3 may not be pushed completely to one side under the conditions of our current measurements. Adding triethylamine (TEA) to the acidified monomer solutions resulted in spectral shifts back to the original positions (Figure 1). These results with the monomers suggest that the electronic properties of their respective polymers may likewise be tuned reversibly in the presence of acid and base.

We were unable to observe UV spectral shifts for **6** or **7** in the presence of (sub-) stoichiometric amounts of TFA (0.1−2.0 equiv) in the course of controlled titration experiments due to the substantial decrease in solution acidity at these concentrations. On the basis of our UV−vis data alone, we cannot formally assign a specific site of protonation for the monomer systems. To shed more light on this issue, we examined the alkylation of **6** and **7** by Meerwein's salt (Et$_3$OBF$_4$) under spectroscopic conditions. No change in absorption profile was noted for **7**, but a noticeable red-shifted absorption similar to that found in the presence of TFA was noted for **6**. Breslow's seminal work established that alkylation of diphenylcyclopropenone occurs at the carbonyl oxygen leading to an isolable ethoxy cyclopropenium cation species.[21] Indeed, we were able to obtain isolable amounts of the aromatic cation **8** through the treatment of a small quantity of **6** with Meerwein's salt followed by removal of the reaction solvent. We can conclude from these experiments that the protonation site for **6** is most likely at the carbonyl, because the UV−vis and NMR spectral properties for **6** in the presence of both TFA and EtO$_3$BF$_4$ showed comparable behavior. For example, the two symmetric β-thiophene protons of **6** (7.73 ppm) assigned as those closest

to the cyclopropenone core became progressively more deshielded in the presence of TFA (7.91 ppm) and on the isolated salt **8** (8.11 ppm). This is consistent with enhanced ring current in the cyclopropenone fragment due to resonance upon protonation/alkylation. Spectral details for these experiments may be found in the Supporting Information.
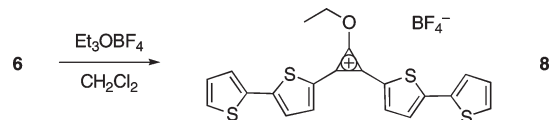

Electropolymerization. All synthesized monomers were subjected to cyclic voltammetry (CV) to observe anodic oxidation and subsequent follow-up polymerization. Cyclopropenone monomers **1**, **3**, and **4** had clearly irreversible CVs, but no polymer growth was observed. It is not clear if this irreversibility is simply due to decomposition of the oxidized species or to solubility of the oligomers generated in the CV experiment that minimize deposition on the electrode surface. Therefore, the remainder of this article will focus on the two monomers that successfully polymerized during CV, bithienyl cyclopropenone **6** and carbonyl **7**.

Cyclopropenone **6** had a peak anodic oxidation potential (E_{pa}) at 0.95 V (Figure 2a, with an onset of anodic current around 0.8 V), a value that was much less positive than that of carbonyl **7** (E_{pa} was approximately 1.4 V, with an onset around 1.2 V, Figure 2b). Having a lower monomer E_{pa} is favorable because it reduces the possibility of overoxidation of the polymer being formed on the electrode. For both **6** and **7**, new oxidation peaks indicative of polymer formation were observed growing in at lower potential. For the cyclopropenone-containing poly(**6**) there appeared to be two new reversible peaks with E_{pa} values at 0.38 and 0.60 V. For the carbonyl-containing polymer poly(**7**) the E_{pa} fell at 1.1 V. Poly(**7**) grew more efficiently than poly(**6**), leading us to suspect that poly(**6**) consisted primarily of small oligomers. Regardless, it is important to recognize that the monomer **6** itself contains 5 unsaturated rings thus providing electrosynthesized polymers of reasonable lengths.

Polymer Cyclic Voltammetry. The polymer CVs were recorded in 0.1 M TBAPF$_6$/CH$_2$Cl$_2$, using polymer-coated Pt button working electrodes (Figure 3). Poly(**6**) had the lower E_{pa} of 0.64 V that was 0.52 V less positive than the E_{pa} of 1.16 V recorded for poly(**7**). The CV of the poly(**6**) also shows a small reversible oxidation prepeak at 0.19 V. The

SCHEME 4. **Resonance Structures That Contribute to the Electronic Properties of Poly(6 (left) and Poly(7 (right) in the Neutral State and upon Treatment with Acid.[a]**
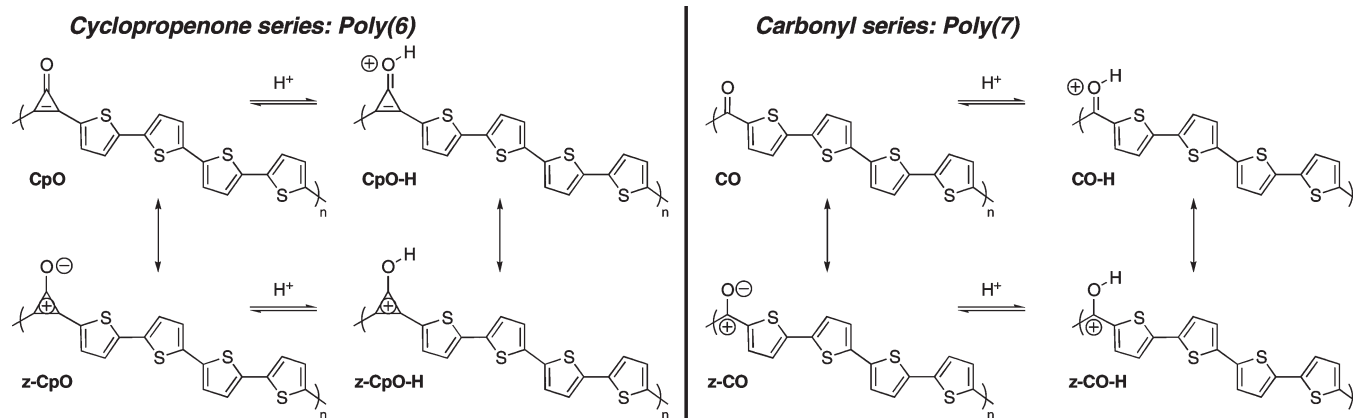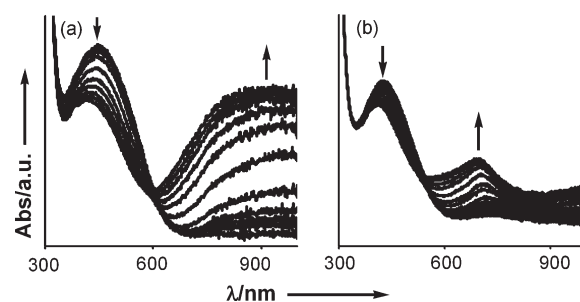

[a]The zwitterionic forms (**z-CpO** and **z-CO**) refer to the charge separated form of the carbonyl as a formal C^+-O^- single bond.
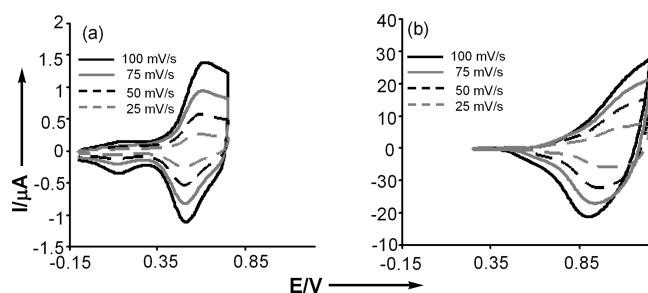
FIGURE 3. Cyclic voltammograms of (a) poly(**6**) and (b) poly(**7**) taken at different scan rates (as indicated) in 0.1 M TBAPF$_6$/CH$_2$Cl$_2$ with use of polymer-coated Pt button working electrodes. All other conditions are as described in Figure 2.

FIGURE 4. Spectroelectrochemical data for (a) poly(**6**) and (b) poly(**7**) obtained in 0.1 M TBAPF$_6$/DCM with use of polymer-coated ITO glass working electrodes. All other conditions are as described in Figure 2.
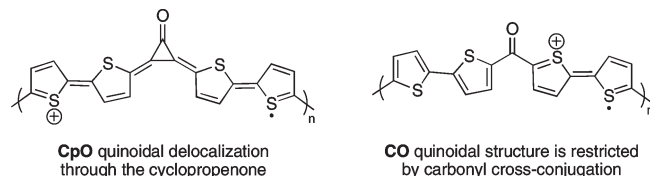
data points to the HOMO of the poly(**6**) being higher than that of the poly(**7**), indicating that the electron-withdrawing nature of the carbonyl unit exerts more of an electronic influence when directly attached to the oligothiophene repeat units within poly(**7**) (structure **CO** in Scheme 4) than as a component of the cyclopropenone ring (structure **CpO** in Scheme 4).

Spectroelectrochemistry. Electrochemical polymerizations of **6** and **7** were carried out on ITO glass electrodes under ambient conditions in 0.1 M TBAPF$_6$/CH$_2$Cl$_2$. This allowed for spectroelectrochemical data to be obtained by taking the UV−visible spectra of the respective polymers immobilized on the ITO support while holding the electrode at different potentials. As was the case for the monomers, the neutral poly(**6**) had a 23 nm longer λ_{max} than poly(**7**) (Figure 4). During oxidation, poly(**6**) showed a broad polaronic peak at 905 nm that started growing when the polymer was held at 0.22 V. Poly(**7**) exhibited a much sharper and higher-energy peak at 693 nm, which did not start growing in until the polymer was held at 0.71 V. The charges in poly(**7**,**CO**) may also be more localized on the thiophenyl portions of the polymer because quinoidal delocalization may be stunted by the cross-conjugation imposed by the carbonyl in the polymer backbone. In both cases, as the applied potential was incrementally increased, persistent spectral signatures corresponding to the pristine or neutral polymer films remained to further suggest localized electronic character. Attempts to

obtain IR signatures of the carbonyls contained within these films using attenuated total reflectance were complicated by excessive absorption in the low-energy region of the spectra arising from what seems to be residual electrolyte trapped in the polymer films.

CpO quinoidal delocalization through the cyclopropenone

CO quinoidal structure is restricted by carbonyl cross-conjugation

Influence of Trifluoroacetic Acid. The addition of TFA to the electrolyte solution in which the CVs of the polymers were recorded resulted in shifts of their anodic processes to higher potentials (Figure 5). It was expected that TFA at sufficiently high concentrations would protonate the cyclopropenone carbonyls of poly(**6**) therefore enforcing a greater contribution of the cyclopropenium cations along the conjugated polymer backbone (**z-CpO-H**, Scheme 4). Likewise, protonation of the carbonyls of poly(**7**) would break the cross-conjugation between the quaterthiophenes in adjacent repeating units (**z-CO-H**, Scheme 4). The more TFA present in the solution, the greater the positive shift in the potential observed for polymer oxidation in both cases. This is most likely due to the introduction of cationic charges into the
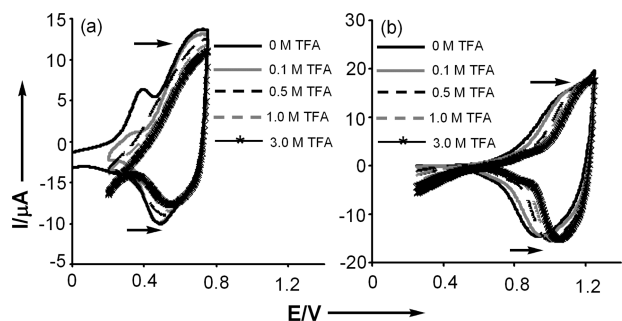
FIGURE 5. Changes in the cyclic voltammograms of (a) poly(**6**) and (b) poly(**7**) as the concentration of TFA in the 0.1 M TBAPF$_6$/CH$_2$Cl$_2$ solution was increased from 0.0 to 3.0 M. All other conditions are as described in Figure 2.

FIGURE 6. UV−visible spectra of (a) poly(**6**) and (b) poly(**7**) deposited on ITO electrodes and recorded in 0.1 M TBAPF$_6$/CH$_2$Cl$_2$. The arrows indicate the spectral changes that occurred upon exposure of the film to 3.0 M TFA.

polymer backbone making oxidation of the polymer more difficult. It was also noted that the small prepeak in the CV of poly(**6**) disappeared upon the addition of TFA but returned upon soaking the polymer film in neutral monomer-free electrolyte.

Polymers deposited onto ITO were also subjected to TFA treatment in order to visualize protonation-induced changes in electronic structure optically. The UV−visible spectra of the polymers were recorded as the concentration of TFA in the electrolyte solution was increased from 0.0 to 3.0 M. For poly(**6**), the effects of protonation proved to be almost unnoticeable, with the appearance of a very weak absorption peak at approximately 950 nm that was buried in the noise of the low-energy region of the spectrum. Increasing the TFA concentration resulted in little or no change to this low-energy absorption but led to a reduction in intensity for the neutral polymer λ_{max} (Figure 6a). When TEA was added to neutralize the acid present, the low-energy peak disappeared while the neutral polymer absorption increased, although not to its original height. For poly(**7**), as the TFA concentration was increased, a new low-energy peak at 735 nm grew progressively more intense accompanied by a reduction in the neutral spectral signature (Figure 6b). The evolution of the low-energy peak mirrored what was observed spectroelectrochemically for poly(**7**) during electrochemical oxidation to generate radical cations and other charged structures (Figure 4b). The addition of an equimolar amount of TEA to the TFA solution resulted in the disappearance of the peak at higher wavelength and an increase in the original peak (although again not back to the original height). Surprisingly, we found no spectral changes for poly(**6**) or poly(**7**) in the presence of Meerwein's salt but noted that the spectral shift for monomer **6** once exposed to Meerwein's salt in electrolyte solution was not as dramatic as that described above (Figures S9−11, Supporting Information).

Although we can in a sense draw analogies from this work to established examples of protonic acid doping leading to mobile carriers and electrically conductive materials,[26−28] in the present case it appears that we are only altering band structure. Protonation of the cyclopropenone carbonyls of poly(**6**) leads to a greater contribution from the resonance structure of the cyclopropenium ion. Therefore, protonation
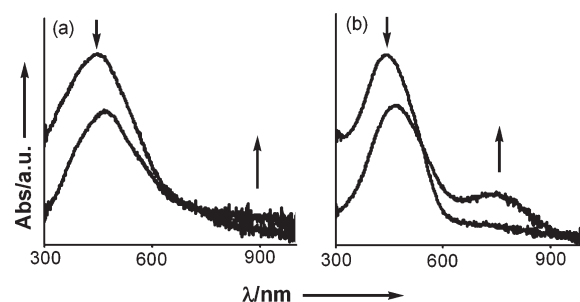
is only inducing a conversion in the polymer electronic structure from an oligothienylene-vinylene to a typical oligoaromatic. The olefinic structure can be thought of as supporting a greater delocalization of radical cations and other charged species, but the cyclopropenium cation might actually restrict extended quinoidal delocalization during polymer oxidation. This is due to the fact that although thiophene and cyclopropenone have comparable NICS values,[29] the cyclopropenium cation has a substantially more negative NICS value (−28.1) relative to cyclopropenone (−18.3) indicating greater aromaticity.[13] The cost to disrupt the cyclopropenium aromaticity in order to access the quinoidal structure should therefore be more energetically unfavorable. Indeed, there are minimal spectroscopic differences between the triphenylcyclopropenium cation and that of the analogous para-substituted benzene bearing two cyclopropenium substituents indicating that the extent of intramolecular delocalization is not enhanced in longer oligomers.[30] On the other hand, poly(**7**) represents a cross-conjugated structure that enables more intramolecular delocalization through the formal vacant p-orbital created upon protonation of the carbonyl that relieves the cross-conjugation delocalization barrier (see structures **z-CpO-H** and **z-CO-H** in Scheme 4). This scenario is analogous to Wudl's work to remove cross-conjugation within pyridine vinylenes through alkylation or protonation.[31]

It is important to consider that in the presence of such high concentrations of TFA, the oligothiophenes along the conjugated backbones may not be innocent bystanders but rather also acted upon by TFA. We recorded the UV−vis spectrum of α-quaterthiophene (α-4T) in 0.5 M TFA and in the presence of Meerwein's salt as was done for monomers **6** and **7** above (Figures S3 and S4, Supporting Information). This monomer was studied due to the presence of the quaterthiophene moiety within poly(**6**) and poly(**7**) formed after oxidative dimerization and polymerization of the respective bithiophene-functionalized monomers. The treatment of α-4T with TFA led to a new absorption at 649 nm with a high-energy shoulder at 619 nm. Although this was quite weak in intensity compared to the persistent signature of neutral α-4T appearing at 389 nm, it is indicative of the formation of α-4T radical cation formed from electron

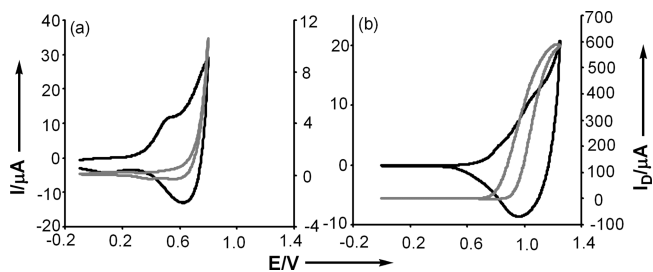(26) Chiang, J. C.; MacDiarmid, A. G. *Synth. Met.* **1986**, *13*, 193−205.
(27) Han, C. C.; Elsenbaumer, R. L. *Synth. Met.* **1989**, *30*, 123−131.
(28) Wang, F.; Lai, Y. H.; Han, M. Y. *Macromolecules* **2004**, *37*, 3222−3230.

(29) Suresh, C. H.; Koga, N. *Chem. Phys. Lett.* **2006**, *419*, 550−556.
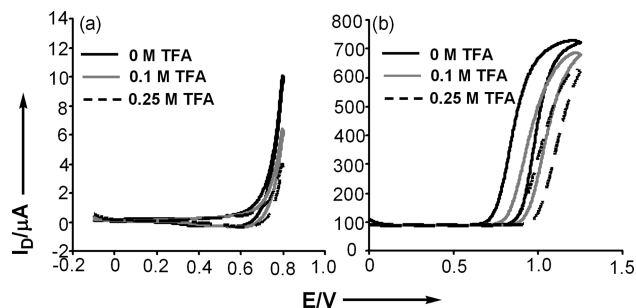(30) Eicher, T.; Berneth, H. *Tetrahedron Lett.* **1973**, 2039−2042.
(31) Wang, H.; Helgeson, R.; Ma, B.; Wudl, F. *J. Org. Chem.* **2000**, *65*, 5862−5867.

FIGURE 7. Conductivity profile (gray) and CV (black) of poly(**6**) (left) and poly(**7**) (right) with the polymer-coated Au interdigitated microelectrode array as the working electrode. The CVs were acquired at 100 mV/s scan rates while the drain current measurements were taken at 5 mV/s scan rates. All other conditions are as described in Figure 2.

FIGURE 8. Conductivity profiles of (a) poly(**6**) and (b) poly(**7**) obtained in 0.1 M TBAPF$_6$/DCM with 0.00, 0.10, or 0.25 M TFA. All other conditions are as described in Figure 2.

transfer between neutral and protonated α-4T.[32] Indeed, Fichou reported the UV−vis of electrochemically generated α-4T radical cation showing absorbance at 645 nm with a high-energy shoulder at 620 nm.[33] In contrast, Meerwein's salt led to no detectable spectral changes in the UV−vis spectrum of α-4T. Therefore, in the case of the polymers, we cannot discount acid-induced protonation or complexation of the formal quaterthiophene moiety of the repeat unit as contributing to the observed electronic properties of poly(**6**) or poly(**7**) in the presence of such large concentrations of TFA. Our results above with **6** in the presence of Meerwein's salt would suggest that the *O*-alkylation (and protonation with TFA) would be the most important (but not necessarily the *only*) contributor to the electronic structure of the polymer under comparable acidic conditions. We should point out that the α-4T unit in poly(**7**) is in direct electronic conjugation with two electron withdrawing (and deactivating) carbonyl groups and as such may be less prone to electrophilic attack/ protonation in the presence of the fairly strong acid.

In Situ Electrical Conductivity. To examine the possibility for creation of the mobile charge carriers within these polymers, in situ electrical conductivity measurements were performed according to the procedures developed by Wrighton.[34] The polymers were electropolymerized onto gold interdigitated microelectrodes to cover the entire array of the device. The potentials of the two working microelectrodes were controlled by using a bipotentiostat while maintaining a 40 mV offset potential between them. The drain currents (I_D) measured between the two working electrodes covered by poly(**6**) did not begin to rise until around 0.60 V, which is well beyond the onset of the prepeak oxidation of the polymer, and it continued to rise until the end of the scan at 0.80 V (taking the film to more positive potentials usually led to polymer degradation). The maximum drain current observed was 12 μA and only decreased slightly with successive scans. Poly(**7**) became conductive at 0.73 V, which is just about the point of the onset of oxidation of the polymer and increased up to 1.25 V where the measurement was concluded (Figure 7b). Measured I_D values around 600 μA were observed. The magnitude of I_D was reproducible when scanning between 0.00 and 1.25 V, but decreased consider-

ably with each subsequent scan when the range was extended to 1.35 V, indicating polymer degradation. We cannot conclude much since the poor growth of poly(**6**) most likely provided for poor and nonuniform coverage of the microelectrode array relative to poly(**7**).

Finally, we investigated the effect of TFA concentration on the conductivity of the polymers. The concentration of TFA present in solution while taking the measurements was increased from 0.00 to 0.25 M while scanning between −0.10 and 0.80 V for poly(**6**) and between 0.00 and 1.25 V for poly(**7**). For poly(**6**), the maximum I_D observed decreased from 12 μA at 0 M TFA to 4.3 μA at 0.25 M TFA (a 66% relative decrease in conductivity, Figure 8a). For poly(**7**), the I_D decreased from 720 μA at 0.00 M TFA to 625 μA at 0.25 M (a 13% relative decrease, Figure 8b). A slight decrease in drain current was observed with each successive scan at any given TFA concentration, so these trends should be viewed as qualitative since the same polymer-coated electrode was used for all measurements.

This is in accordance with the electrochemical and UV−vis absorption data obtained for TFA protonation presented above. Upon the addition of TFA, the carbonyl of the cyclopropenone is protonated leading to the contribution from the aromatic cyclopropenium cation. The stability gained from this means that the charge does not delocalize as readily (via quinoidal electronic structures) and hence the observed reduction in conductivity is due to either decreased *numbers* or *mobilities* of extended charge carriers. This type of behavior was also observed for fused polycyclic tropone-containing polymers that were previously synthesized by Swager.[24] There is a rich reactivity associated with these polymers, and we plan to study their spin properties in the presence of strong acids and alkylating agents in order to better understand the origins of these effects and to determine the extent of participation of formal cyclopropenium cations versus other electronic alterations.

Conclusions

We have described the synthesis and characterization of a series of thienyl-substituted cyclopropenones as precursors to new electronic materials. From this pool of molecules, we electrochemically synthesized and studied a conductive organic polymer poly(**6**) that formally incorporates the smallest Hückel aromatic, the cyclopropenium cation. The electronic properties of poly(**6**) could be controlled by protonation but in a way opposite to what is typically observed in acid doping. Here, protonation of the polymer results in a

(32) Davies, A. G. *J. Chem. Res. (S)* **2001**, 253–261.

(33) Fichou, D.; Horowitz, G.; Xu, B.; Garnier, F. *Synth. Met.* **1990**, *39*, 243–259.

(34) Ofer, D.; Crooks, R. M.; Wrighton, M. S. *J. Am. Chem. Soc.* **1990**, *112*, 7869–7879.

reduction of the apparent conductivity due to the increased influence of the aromatic cyclopropenium cation that is energetically resistant to the formation of extended quinoidal structures. Thus, the mobilities and/or the densities of charge carriers can be controlled externally through protonation in a manner that fundamentally alters the electronic structure of the polymer backbone rather than, for example, self-doped polymers generated through protonating or alkylating pendant ionizable groups attached to solubilizing side chains. We are currently exploring chemically synthesized materials derived from bromo **2** and hexyl **3** and will report this work as it matures.

Experimental Section

General Considerations. Thiophene, 2-bromothiophene, 3-hexylthiophene, 3-methoxythiophene, 2-methylthiophene, bithiophene, dimethylcarbamyl chloride, thionyl chloride, aluminum trichloride ($AlCl_3$), tetrachlorocyclopropene (C_3Cl_4), N-bromosuccinimide (NBS), Meerwein's salt (Et_3OBF_4), acetic acid, trifluoroacetic acid, and n-butyllithium (n-BuLi) (1.6 M in hexane) were obtained commercially and used without further purification. Tetrahydrofuran (THF) and dichloromethane (DCM) were dispensed after being pushed through two columns of activated alumina. ^{1}H NMR and ^{13}C NMR were obtained in $CDCl_3$ at 400 and 100 MHz, respectively, on an FT-NMR spectrometer. Chemical shifts are reported in parts per million relative to residual protio solvent [$CHCl_3$, 7.24 (^{1}H) and 77.00 ppm (^{13}C)].

UV–Visible Spectroscopy. For each monomer, a solution of approximately 3×10^{-6} M in chloroform was used for obtaining the UV–visible spectra at room temperature.

IR Spectroscopy. For each monomer, a solution was prepared in spectrophotometric grade chloroform. The solution was dropcasted onto a KBr plate. A background reading was taken and then the IR spectrum was recorded on an FT-IR spectrophotometer.

Electrochemical Methods. Cyclic voltammetry (CV) and electrochemical polymerizations were carried out with a potentiostat. A 1.6 mm diameter platinum button was used as the working electrode for CV. A Pt wire was used as the counter electrode and an Ag wire in 0.01 M $AgNO_3$ in 0.1 M tetrabutylammonium hexafluorophosphate ($TBAPF_6$) in acetonitrile (ACN) was used as the quasi-internal reference electrode. All electrochemical potentials are reported and discussed relative to this reference electrode. Scans were performed at 100 mV/s. Dichloromethane was dispensed after being pushed through two columns of activated alumina. $TBAPF_6$ was obtained commercially and recrystallized from ethanol prior to use. All $TBAPF_6$ electrolyte concentrations were 0.1 M in DCM and monomer concentrations were 2.5–5 mM.

Qualitative in situ conductivity was also obtained with a bipotentiostat. The working electrode was an Au 5 μm interdigitated microelectrode array and the counter and reference electrodes were the same as those mentioned above. Polymers were electropolymerized on the Au microelectrode devices from 5 mM monomer solutions in 0.1 M $TBAPF_6$/DCM. The cyclic voltammograms of the polymers were then recorded in monomer free electrolyte solution. Finally, drain currents were measured within the same potential range as the CVs were measured. A potential difference of 40 mV was applied between the two scanning working electrodes, and a scan rate of 5 mV/s was used.[34]

Spectroelectrochemical Measurements. Electropolymerization of the monomers was done with 70–100 Ω/sq surface resistivity indium-doped tin oxide coated glass electrode (ITO) as the working electrode and 0.1 M $TBAPF_6$/DCM as the electrolyte. The polymer-coated ITO was rinsed with fresh electrolyte and placed in a quartz cuvette containing blank electrolyte with counter and reference electrodes similar to those described above for CV. While varying the potential at which the polymer was held, the UV–visible spectra were recorded with a UV–vis spectrophotometer. A baseline of ITO in monomer-free electrolyte was used.

Theoretical Calculations. Density functional theory (B3LYP/6-31G*) was employed in Spartan with energy-minimized structures to determine the HOMO and LUMO energy levels of the monomers.

Monomer Synthesis. Representative procedures for cyclopropenone and carbonyl monomers, full experimental details, and characterization data for monomers **1**, **2**, **3**, and **4** can be found in the Supporting Information.

2,3-Di(2,2′-bithiophen-5-yl)cycloprop-2-enone (6). To a 25 mL Schlenk flask was added $AlCl_3$ (85 mg, 0.64 mmol), and the flask was evacuated and refilled with nitrogen (3×). Dry DCM (1 mL) was added to form a suspension. The reaction was cooled in an ice bath and then C_3Cl_4 (102 mg, 0.57 mmol) was added. The reaction was allowed to stir for 15 min, and a solution of bithiophene (207 mg, 1.3 mmol) in DCM (0.5 mL) was added at once. The reaction was allowed to stir for 45 min while being kept in the ice bath, after which the reaction was quenched slowly by the addition of water. The reaction mixture was filtered, and the filtrate was transferred to a separatory funnel. The organic layer was collected and the aqueous layer was extracted with DCM. The organic layers were combined and dried over $MgSO_4$. The mixture was filtered and the solvent was evaporated to provide a red solid. The product was purified initially on a silica plug and further by column chromatography with 1:5 ether/DCM as the eluent. The solvent was evaporated to obtain an orange solid (63 mg, 0.16 mmol, 29%). ^{1}H NMR (300 MHz, $CDCl_3$) δ (ppm) 7.73 (d, J = 4.0 Hz, 2H), 7.33 (m, 4H), 7.31 (d, J = 4.0 Hz, 2H), 7.10 (m, 2H); ^{13}C NMR (100 MHz, $CDCl_3$) δ (ppm) 149.3, 145.6, 136.4, 135.9, 128.3, 126.8, 125.8, 125.1, 124.4, 123.3; HRMS (FAB) calcd for $C_{19}H_{11}OS_4$ [MH^+] 382.9693, found 382.9685; IR (KBr) ν (cm^{-1}) 3378, 3030, 2927, 2858, 2781, 1843, 1829, 1772, 1751, 1724, 1700, 1653, 1606, 1539, 1506, 1447, 1399, 1053, 792, 536.

Di-2,2′-bithiophen-5-ylmethanone (7).[18] To a 100 mL Schlenk tube that had been flame-dried and cooled under N_2 was added bithiophene (2.51 g, 15 mmol). The flask was evacuated and refilled with N_2 (3×). THF (20 mL) was added to the flask. The solution was then cooled in an acetone–dry ice bath. n-BuLi (10 mL, 15 mmol) was added dropwise to the reaction mixture and the reaction was allowed to stir for 1.25 h in the ice bath. Then, dimethylcarbamyl chloride (810 mg, 7.5 mmol) was added to the reaction mixture. The reaction was allowed to warm to room temperature and stirred overnight. The reaction was quenched with water. The formation of a precipitate was noted. The mixture was filtered and a yellow-orange solid was collected (1.9 g, 5.0 mmol, 70%). ^{1}H NMR (400 MHz, $CDCl_3$) δ (ppm) 7.82 (d, J = 4.0 Hz, 2H), 7.35 (two apparent doublets, 4H), 7.24 (d, J = 4.0 Hz, 2H), 7.08 (m, 2H); HRMS (FAB) calcd for $C_{17}H_{11}OS_4$ [MH^+] 357.9614, found 357.9612.

Supporting Information Available: Additional synthetic details and characterization data, UV–vis spectra, CVs, and ^{1}H and ^{13}C NMR spectra for all new molecular compounds. This material is available free of charge via the Internet at http://pubs.acs.org.